$Fe@Fe_2O_3$ Core−Shell Nanowires as Iron Reagent. 1. Efficient Degradation of Rhodamine B by a Novel Sono-Fenton Process

Zhihui Ai,[†] Lirong Lu,[†] Jinpo Li,[†] Lizhi Zhang,*[,†] Jianrong Qiu,[‡] and Minghu Wu[§]

Key Laboratory of Pesticide & Chemical Biology of Ministry of Education, College of Chemistry, Central China Normal University, Wuhan 430079, People's Republic of China, National Coal Combustion Laboratory, Huazhong University of Science and Technology, Wuhan 430074, People's Republic of China, and Department of Biology & Chemistry, Xianning College, Xianning 437100, People's Republic of China

Received: August 28, 2006; In Final Form: December 11, 2006

In this study, $Fe@Fe_2O_3$ core−shell nanowires were first used as a novel Fenton iron reagent. The nanowires were synthesized through the reduction of ferric chloride aqueous solution by sodium borohydride at ambient atmosphere, without protection of inert gases or vacuum. Rhodamine B (RhB) could be efficiently degraded in aqueous media by a novel sonochemical-assisted Fenton (sono-Fenton) system based on these $Fe@Fe_2O_3$ core−shell nanowires. The RhB degradation processes were monitored by UV−vis spectroscopy and total organic carbon (TOC) analysis. $Fe@Fe_2O_3$ core−shell nanowires showed much higher activity in the sono-Fenton system than other iron reagents such as commercial zerovalent iron powders (Fe^0), ferrous ions (Fe^{2+}), and ferric ions (Fe^{3+}). It was found that near 100% decoloration and over 60% TOC removal of RhB (5 $mg \cdot L^{-1}$) could be achieved in 60 min by this novel sono-Fenton system with 0.018 $mol \cdot L^{-1}$ $Fe@Fe_2O_3$ core−shell nanowires. This new iron reagents before and after the sono-Fenton reaction were examined by X-ray diffraction (XRD), scanning electron microscopy (SEM), and transmission electron microscopy (TEM). The characterizations found that the nanowires were transferred to nanotubes/nanoparticles covered with Fe_3O_4/Fe_2O_3 after the sono-Fenton process. A possible mechanism of sono-Fenton degradation of RhB with $Fe@Fe_2O_3$ nanowires was proposed on the basis of the experimental results. It involved homogeneous Fenton and heterogeneous Fenton oxidative degradation simultaneously. The high activity of core−shell $Fe@Fe_2O_3$ nanowires and the success of their mass production make them attractive for the treatment of organic pollutants in water.

Introduction

In recent years, advanced oxidation processes (AOPs), which involved an in situ generation of highly potent chemical oxidants such as hydroxyl radicals ($^{\bullet}OH$), have emerged as an important class of technologies to accelerate the nonselective oxidation.[1] Among AOPs, Fenton and sonochemical reactions are widely used for the destruction of recalcitrant organic contaminants in wastewater that cannot be eliminated biologically.

The classic Fenton reagent is commonly referred to the combination of Fe^{2+} and H_2O_2 (Fe^{2+}/H_2O_2). The combination of Fe^{3+} and H_2O_2 is known as Fenton-like reagent (Fe^{3+}/H_2O_2). As Fe^{3+} can be produced from Fenton reagent during reactions, Fenton chemistry and Fenton-like chemistry often occur simultaneously.[2,3] The following reactions show the mechanism of $^{\bullet}OH$ formed when either Fe^{2+} or Fe^{3+} is present (eqs 1 to 5).[4,5]

$$Fe^{2+} + H_2O_2 \rightarrow Fe^{3+} + {}^{\bullet}OH + OH^- \quad (1)$$

$$Fe^{3+} + H_2O_2 \rightarrow Fe(HO_2)^{2+} + H^+ \quad (2)$$

$$Fe(HO_2)^{2+} \rightarrow Fe^{2+} + HO_2 \quad (3)$$

$$O_2^- + Fe^{3+} \rightarrow Fe^{2+} + O_2 \quad (4)$$

$$^{\bullet}OH + H_2O_2 \rightarrow HO_2 + H_2O \quad (5)$$

Although Fenton and Fenton-like reagents (Fe^{3+}/H_2O_2, Fe^{2+}/H_2O_2) are efficient to generate oxidative radicals such as $^{\bullet}OH$ in homogeneous reactions to oxidize organic compounds to CO_2 and water, they have two main drawbacks for the application on a large scale: high cost of H_2O_2 and narrow working pH range. It is known that iron in its ferrous and ferric form requires a working pH <4. At higher pH values, iron precipitates as a hydroxide. Recently, researchers have made great efforts to overcome these drawbacks. One way was to develop a heterogeneous Fenton system containing solid iron phases and H_2O_2.[5,6] For example, supported or immobilized Fenton catalysts were used. These catalysts included Nafion membranes,[7,8] Fe-silica structured surfaces,[9] Fe(III)-loaded resin,[10] Fe_2O_3 immobilized on polyethylene copolymers,[11] alginate microcapsules encapsulated Fe,[12] structured C-Nafion/Fe-ion surfaces,[13] and Fe-histidine complex immobilized on Nafion.[14] The utilizations of these Fenton catalysts can extend the working range of Fenton reaction to a 2−10 pH range; the other way was to develop some combination of technologies such as the photoassisted Fenton process, the electrochemical-assisted Fenton process, and

* Address correspondence to this author. E-mail: zhanglz@mail.ccnu.edu.cn. Phone/fax: +86-27-6786 7535.
[†] Central China Normal University.
[‡] Huazhong University of Science and Technology.
[§] Xianning College.

10.1021/jp065559l CCC: $37.00
Published on Web 03/01/2007

the sonochemical-assisted Fenton process to enhance the generation of hydroxyl radicals, and thus reduce the consumption of H_2O_2.

The sonochemical reaction is another AOP process. When an aqueous solution is exposed to ultrasound irradiation, large pressure gradients occur within the liquid causing the transient expansion and rarefaction of microsized bubbles. This leads to localized spots of high temperatures and pressures within the liquid. Hydroxyl radicals that are formed during the cleavage of water molecules within the cavitations upon collapse can attack many environmental pollutants. Furthermore, the extreme temperatures produced within the microcavity may directly degrade organic pollutants.[15] The ultrasound-induced splitting of water molecules will cause reactions 6−15 in the presence of dissolved oxygen in bulk solution.

$$H_2O \rightarrow {}^{\bullet}OH + H^{\bullet} \quad (6)$$

$$H^{\bullet} + {}^{\bullet}OH \rightarrow H_2O \quad (7)$$

$$H^{\bullet} + O_2 \rightarrow HO_2^{\bullet} \quad (8)$$

$$2{}^{\bullet}OH \rightarrow H_2O_2 \quad (9)$$

$$2HO_2^{\bullet} \rightarrow H_2O_2 + O_2 \quad (10a)$$

$$HO_2^{\bullet} + {}^{\bullet}O_2^{-} + H^{+} \rightarrow H_2O_2 + O_2 \quad (10b)$$

$$HO_2^{\bullet} + {}^{\bullet}OH \rightarrow H_2O + O_2 \quad (11a)$$

$${}^{\bullet}O_2^{-} + {}^{\bullet}OH \rightarrow OH^{-} + O_2 \quad (11b)$$

$$H_2O_2 + {}^{\bullet}OH \rightarrow H_2O + HO_2^{\bullet} \quad (12)$$

$$H_2O_2 + H^{\bullet} \rightarrow {}^{\bullet}OH + H_2O \quad (13)$$

$$O_2 \rightarrow 2O \quad (14)$$

$$O + H_2O \rightarrow 2{}^{\bullet}OH \quad (15)$$

Moreover, Fe^0 reductive technology is an innovative and emerging technology in environmental remediation. For example, Fe^0 was used to remove organic compounds and some poisonous metals in groundwater or soil.[16−24] In addition, iron oxides such as magnetite (Fe_3O_4) and maghemite (Fe_2O_3) were also used to catalyze degradation of H_2O_2 or organic pollutants in the environment.[25] Most previous studies concentrated on sono-Fenton reaction with Fe^{2+} or Fe^{3+} as the iron reagent. Only a few reports investigated the Fenton system based on Fe^0 or iron oxide.[26]

In this study, for the first time $Fe@Fe_2O_3$ core−shell nanowires were used as an iron reagent in the sono-Fenton reaction. It is interesting to find that the sono-Fenton system with $Fe@Fe_2O_3$ core−shell nanowires shows excellent efficiency for the degradation of RhB in aqueous solution, which provides an attractive system for the treatment of organic pollutants in water.

Experimental Section

Reagents. All reagents were of analytical grade and were used without further purification.

Synthesis of $Fe@Fe_2O_3$ Core−Shell Nanowires. The nanowires were synthesized by reaction between ferric chloride and sodium borohydride, which was slightly modified from the method reported in our previous study.[27] In a typical procedure, 0.15 g of $FeCl_3{\cdot}6H_2O$ and 0.3 g of $NaBH_4$ were dissolved in 50 mL and 20 mL of deionized water, respectively. Then, the resulting $NaBH_4$ solution was dropped into the $FeCl_3{\cdot}6H_2O$ solution in a 150-mL flask. The addition rate of $NaBH_4$ was about 0.2 mL/s. The whole synthesis process was performed at ambient atmosphere, without protection of inert gases or vacuum. The flask was shaken by hand (magnetic stirring could not be used to avoid magnetically induced aggregation of the resultant iron particles) during the addition. The solution bubbled plenty of gas with the addition of $NaBH_4$ solution, accompanying by fluffy black precipitates appearing on the surface of the solution. The fluffy black precipitates were collected and then washed with deionized water and ethanol, and finally dried under nitrogen flow for characterization and use. The whole procedure could be scaled up to produce $Fe@Fe_2O_3$ core−shell nanowires in tens of grams.

Procedure of Sono-Fenton Reactions. The sono-Fenton experiments were carried out in an ultrasound clean bath with frequency of 25 kHz (100 W, KQ-100A, China). The initial pH value of the RhB solution was adjusted to 2 with 0.1 M H_2SO_4. In some cases, neutral pH was also used without addition of H_2SO_4. First 0.9 mmol of $Fe@Fe_2O_3$ nanowires (the molecular weight of nanowires was assumed as 56) was introduced into 50 mL of 5 $mg{\cdot}L^{-1}$ RhB solution in a 100-mL glass cell with a water cooling jacket outside. Air was bubbled (0.1 $m^3\ h^{-1}$) into the RhB solution during the sono-Fenton degradation. As a comparison, experiments with ultrasound irradiation alone, the sono-Fenton process with 0.9 mmol of commercial Fe^0, Fe^{2+}, or Fe^{3+} as iron sources, were conducted under the same conditions, respectively. The concentration of RhB was monitored by colorimetry with a U-3310 UV−vis spectrometer (HITACHI) at an interval of 10 min. TOC analysis during the degradation of RhB was performed with an Apollo 9000 TOC analyzer (Techcomp).

Characterization of the Freshly Prepared and Used $Fe@Fe_2O_3$ Nanowires. X-ray powder diffraction patterns of the samples were obtained on a Bruker D8 Advance X-ray diffractometer with Cu Ka radiation ($\lambda = 1.54178$ Å). Scanning electron microscopy images were performed on a LEO 1450VP scanning electron microscope. Transmission electron microscopy images were recorded on a Tecnai 20 FEG transmission electron microscope.

Measurements of Hydrogen Peroxide and Total Iron Ion Concentrations. The analysis of hydrogen peroxide was carried out by using the UV−vis spectrum and off-line sampling.[28] First 0.75 mL of 1,2-benzenedicarboxylic acid (0.1 $mol{\cdot}L^{-1}$) was mixed with 0.75 mL of an aqueous solution containing 0.4 $mol{\cdot}L^{-1}$ potassium iodide, 0.06 $mol{\cdot}L^{-1}$ sodium hydroxide, and 1×10^{-4} $mol{\cdot}L^{-1}$ ammoniummolybdate, followed by addition of 1.5 mL of sample solution. After standing for 2 min, the resulting mixed solution was analyzed with a UV−vis spectrophotometer (U-3310, HITACHI) by measuring the absorbance at 352 nm where the absorbance was linearly dependent on H_2O_2 concentration in the solution. The concentration of total iron ions (Fe^{2+} and Fe^{3+}) in the solution was measured by atom absorption spectrometry (WFX-1F2, China).

Results and Discussion

Characterization of $Fe@Fe_2O_3$ Core−Shell Nanowires. A typical XRD pattern (Figure 1) of the as-prepared sample matches well with the standard patterns of cubic Fe (JCPDS file No. 3-1050) and Fe_2O_3 phase (Hematite, JCPDS file No.

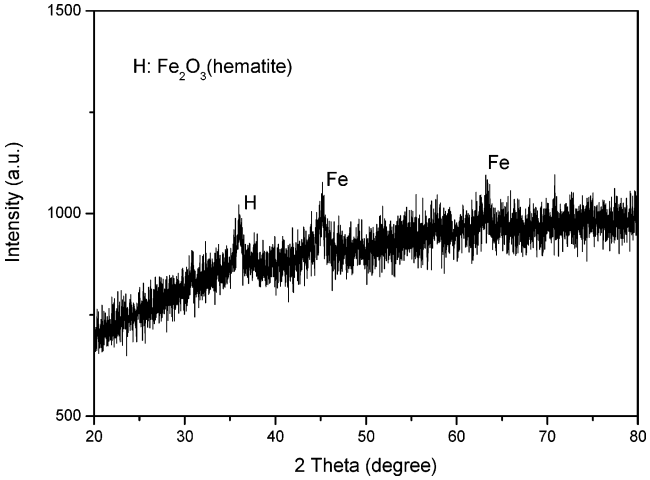

Figure 1. XRD pattern of the as-prepared sample.

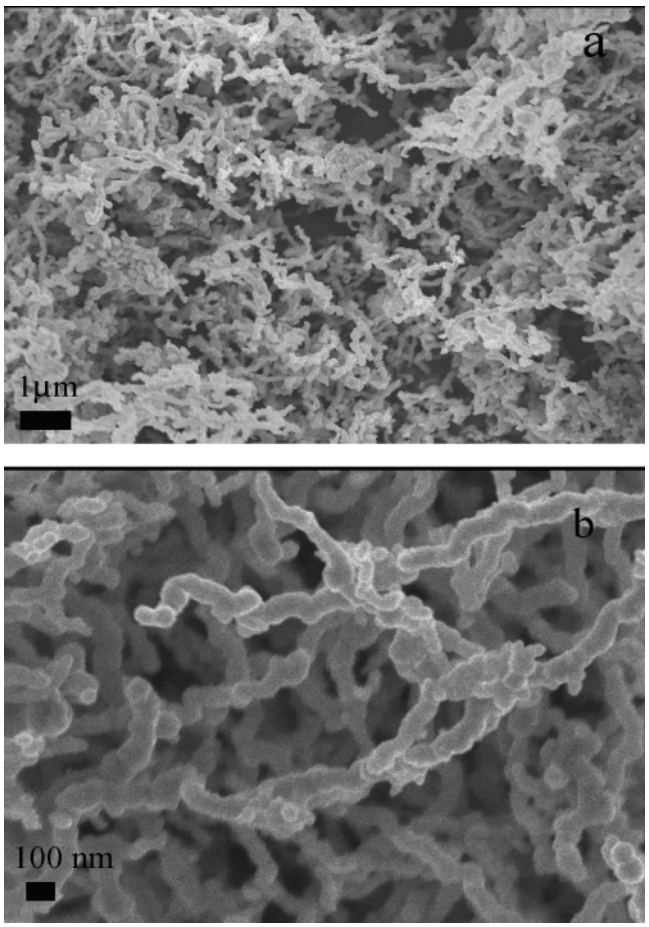

Figure 2. The SEM images at low magnification (a) and high magnification (b) of the as-prepared sample.

2-915). It reveals that Fe and Fe_2O_3 coexist in the as-prepared sample. The SEM image shows that the as-prepared product is of numerous wire-like structures with about 100% ratio (Figure 2a). A high-magnification SEM image reveals that the diameters of the nanowires are about 80 nm (Figure 2b). TEM images of the nanowires clearly reveal the contrast between the gray edge and the dark center of the nanowire, suggesting the core−shell structure of the nanowires (Figure 3). The diameters of the core−shell nanowires are about 80 nm, consistent with the SEM observation. The thicknesses of shells are about 10 to 40 nm according to TEM images. Combining with the results of XRD analysis, we assigned the shells to Fe_2O_3, which were produced

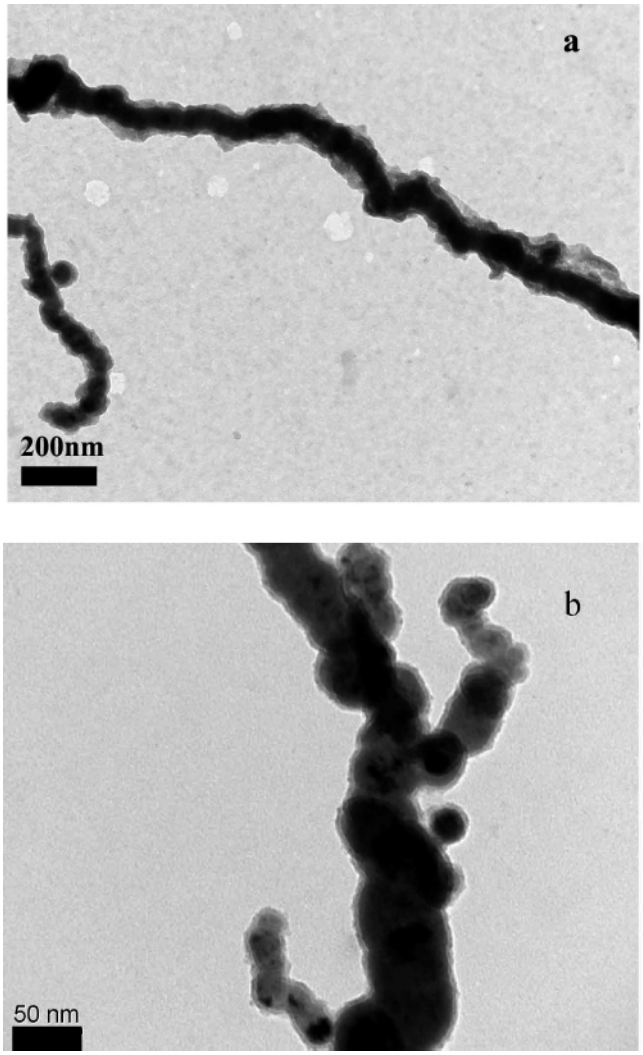

Figure 3. The TEM images of the as-prepared Fe@Fe_2O_3 core−shell nanowires.

by the oxidation of Fe cores during the synthesis and transportation. Therefore, we concluded that the as-prepared sample consisted of Fe@Fe_2O_3 core−shell nanowires. These core−shell Fe@Fe_2O_3 nanowires were very stable in air because of the protection of oxide shells. Their stability made it possible to apply them to an environmental remedy.

RhB Decolaration and TOC Removal in Different Sono-Fenton Processes. Because of its strong absorption in the visible light region and excellent stability under various pH values, RhB was chosen as a model dye pollutant to examine a new sono-Fenton system with these Fe@Fe_2O_3 nanowires as the iron reagent. For comparison, experiments were also performed with ultrasound alone (sono), ultrasound and commercial Fe^0 (sono-Fe^0), ultrasound and Fe^{2+} (sono-Fe^{2+}), ultrasound and Fe^{3+} (sono-Fe^{3+}), and ultrasound and Fe@Fe_2O_3 (sono-Fe@Fe_2O_3), respectively.

Figure 4 displays the temporal absorption spectrum changes of RhB degraded by the sono-Fe@Fe_2O_3 process. The characteristic absorption band of RhB at about 555 nm decreased rapidly and almost disappeared after reaction for 30 min. Meanwhile, the color of the reaction solution changed from the initial pink-red to almost colorless. The RhB degradation often occurs via two competitive processes: one is N-demethylation and the other is the destruction of the conjugated xanthene structure (the chromophores). It is recognized that the decrease of the absorption band of RhB at 555 nm corresponds to the

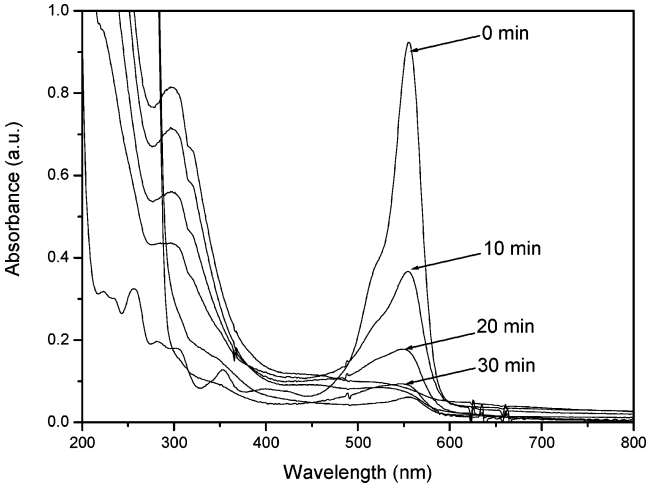

Figure 4. UV−vis spectral changes of RhB as a function of reaction time during the sono-Fe@Fe_2O_3 process. The initial concentration of RhB was 5 mg·L^{-1}, pH 2, the initial concentration of Fe@Fe_2O_3 was 0.018 mol·L^{-1}.

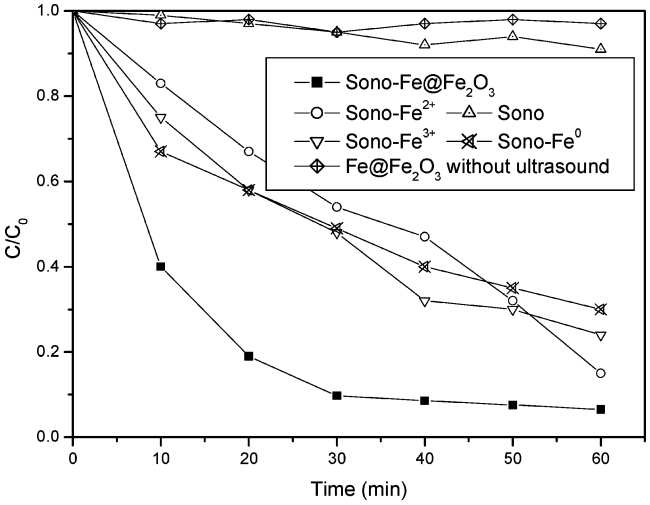

Figure 5. Degradation of RhB as a function of reaction time during different processes. The initial concentration of RhB was 5 mg·L^{-1}, pH 2, the initial concentrations of iron reagents were 0.018 mol·L^{-1}.

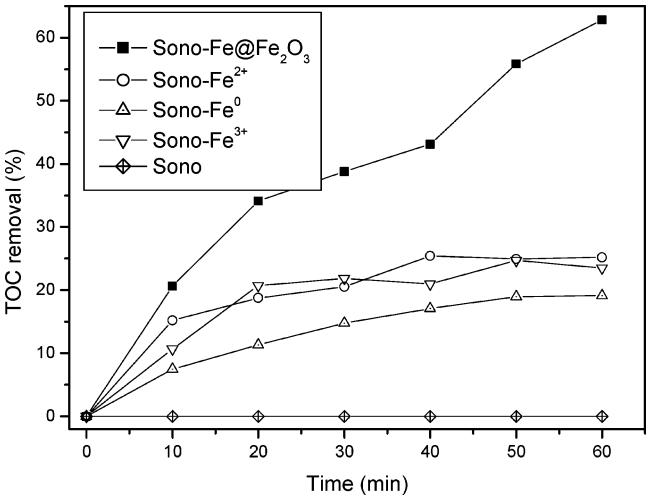

Figure 6. Temporal changes of TOC during the degradation of RhB. The initial concentration of RhB was 5 mg·L^{-1}, pH 2, the initial concentrations of iron reagents were 0.018 mol·L^{-1}.

decomposition of the conjugated xanthene ring in RhB, while the absorbance spectra at 555 nm shifting toward the blue region suggests the de-ethylated RhB molecule formed.[29] In our case, no obvious blue-shift of absorbance at 555 nm was observed. Therefore, the sono-Fenton degradation of RhB with Fe@Fe_2O_3 nanowires was attributed to the destruction of the conjugated structure. It was thought that •OH radicals were added to C−N bonds of the chromophores, replacing the aryl bonds. Moreover, a new absorption peak near 300 nm appeared after 10 min of degradation, indicating some intermediates such as *N*-de-ethylation, cyclohexane, 1,3-dicyclohexylurea, and piperidine were produced.[30,31] This new absorbance also decreased with prolonged reaction time and disappeared after 50 min, which revealed the complete destructions of these intermediate products.

The pH value of the solution increased sharply (from the initial pH 2 to 6) within 10 min and remained constant at 6 during the subsequent sono-Fe@Fe_2O_3 process. The increase of pH value indicated that Fe@Fe_2O_3 core−shell nanowires reacted with H^+ according to reactions 16−18. These reactions would release Fe^{3+} and/or Fe^{2+} under acidic condition. Moreover, reactions 18 and 19 might take place because of the dissolved oxygen in solution, which also increases the pH value. Similarly, when the RhB solution was degraded by the sono-Fe^0 process, the pH value also increased from the initial 2 to 6, which indicated Fe^0 was dissolved in acid condition or oxidized by water and oxygen according to reactions 17−19. However, during the sono, sono-Fe^{2+}, and sono-Fe^{3+} processes, pH values of the solutions did not change because reactions 16−19 would not occur.

$$Fe_2O_3 + 6H^+ \rightarrow 2Fe^{3+} + 3H_2O \quad (E_H^0 = 0.728\ V) \tag{16}$$

$$Fe^0 + 2H^+ \rightarrow Fe^{2+} + H_2 \quad (E_H^0 = -0.440\ V) \tag{17}$$

$$Fe^0 + 2H_2O \rightarrow Fe^{2+} + H_2 + OH^- \tag{18}$$

$$2Fe^0 + O_2 + 2H_2O \rightarrow 2Fe^{2+} + 4OH^- \tag{19}$$

Figure 5 shows the temporal concentration changes of RhB in different processes. Results indicated that neither ultrasound nor Fe@Fe_2O_3 alone could effectively degrade RhB. The degradation of RhB became obvious in the presence of iron reagents such as Fe^{2+}, Fe^{3+}, Fe^0 or Fe@Fe_2O_3. For 50 mL of 5 mg/L RhB solution, 46%, 52%, and 51% degradation rates was obtained for the sono-Fe^{2+}, sono-Fe^{3+}, and sono-Fe^0 processes in 30 min, respectively, while a 90% degradation rate was obtained for the sono-Fe@Fe_2O_3 process in 30 min. The degradation rates were 85% for the sono-Fe^{2+} process, 76% for the sono-Fe^{3+} process, 70% for the sono-Fe^0 process, and almost 100% for the sono-Fe@Fe_2O_3 process in 60 min, respectively. Therefore, Fe@Fe_2O_3 nanowires were a superior iron reagent in the sono-Fenton system for wastewater treatment. The temporal changes of TOC during the degradation of RhB were shown in Figure 6. Over 60% TOC removal was obtained within 60 min for the sono-Fe@Fe_2O_3 process, while TOC removal rates were 24.1%, 23.5%, and 19.1% for sono-Fe^{2+}, sono-Fe^{3+}, and sono-Fe^0 systems, respectively. The results of TOC removal were consistent with decoloration results. However, the TOC measurements showed that complete mineralization (conversion of all carbon atoms to CO or CO_2) could not be achieved, although a complete decolorization occurred in 60 min for the sono-Fe@Fe_2O_3 system. This meant that some organic compounds still remained when the chromophores were completely broken.

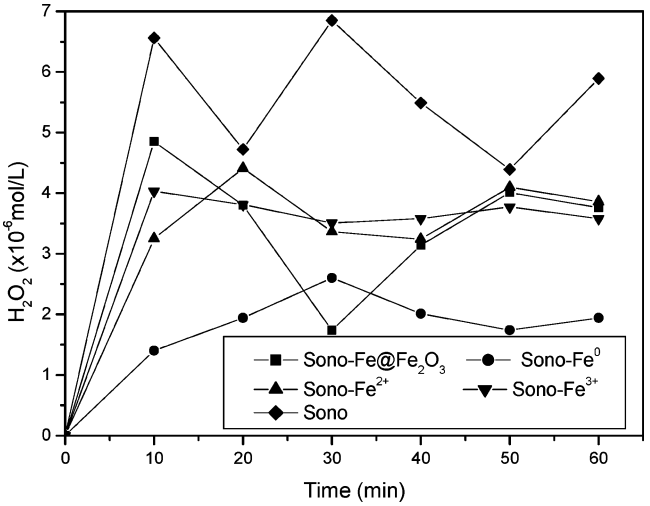

Figure 7. Concentration of hydrogen peroxide as a function of the reaction time. The initial concentration of RhB was 5 mg·L^{-1}, pH 2, the initial concentrations of iron reagents were 0.018 mol·L^{-1}.

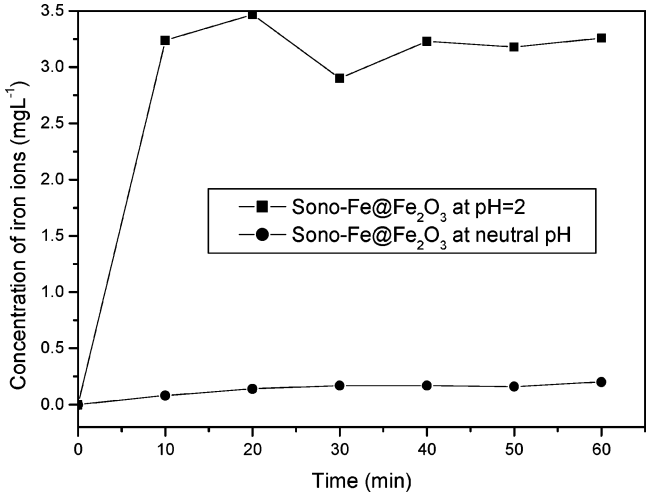

Figure 8. Concentration of iron ions as a function of the reaction time. The initial concentration of RhB was 5 mg·L^{-1}, pH 2, the initial concentration of Fe@Fe_2O_3 core−shell nanowires was 0.018 mol·L^{-1}.

Characterizations of the Used Fe@Fe_2O_3 "Nanowires". The XRD patterns of Fe@Fe_2O_3 "nanowires" used after 30 and 60 min reactions in the sono-Fe@Fe_2O_3 process are somewhat similar (Figure S1, Supporting Information). It was found that Fe_3O_4 (Magnetite, JCPDS file No. 88-866) phase and Fe_2O_3 (Hematite, JCPDS file No. 2-915) phase coexisted in the used Fe@Fe_2O_3 core−shell "nanowires". No peaks from Fe could be observed in the XRD patterns. However, this XRD result did not mean that all of the Fe cores in Fe@Fe_2O_3 nanowires were transformed into iron oxides. This was because we found there were still some commercial Fe^0 particles remaining after 60 min reaction in the sono-Fe^0 process and the molar amount of Fe@Fe_2O_3 nanowires was the same as that of Fe^0 before the sono-Fenton reactions. The reason for no peaks from Fe in the used Fe@Fe_2O_3 "nanowires" could be attributed to the shielding effect of iron oxides on the surface. Therefore, we thought Fe in Fe@Fe_2O_3 nanowires were partially converted into magnetite/hematite.

The used Fe@Fe_2O_3 "nanowires" were further examined by SEM. Their morphology was evidently changed and the nanowires were broken down after the sono-Fe@Fe_2O_3 process (see Figure S2, Supporting Information). Interestingly, some nanotubes were found. This was because some Fe cores of some nanowires were dissolved into ferrous or ferric ions and iron oxide was further deposited on the surfaces of these nanowires from these dissolved iron ions during the sono-Fenton process.[32,33] This further deposition was proved by the larger diameters of these nanotubes than those of the fresh Fe@Fe_2O_3 nanowires. The morphology of the used Fe@Fe_2O_3 "nanowires" was further investigated by TEM. It was found the Fe@Fe_2O_3 nanowires were broken into chainlike nanoparticle superstructures or randomly aggregated nanoparticles (see Figure S3, Supporting Information) after the sono-Fe@Fe_2O_3 reactions. No nanotubes could be found in the TEM images, indicating the nanotubes observed in the SEM images may be destroyed by ultrasound irradiation during the preparation of TEM samples.

Hydrogen Peroxide (H_2O_2) Formation in Different Systems. The RhB aqueous solutions were sampled at an interval of 10 min to measure the concentrations of hydrogen peroxide formed in different processes (Figure 7). It could be observed that the generation of hydrogen peroxide did not increase linearly as the reaction proceeds. The concentration of hydrogen peroxide changed like waves during the process. This is because the •-OH radical is a very reactive species. It cannot only accumulate in solution, but also react with other species. It seemed that the amount of produced H_2O_2 in the sono process was always more than those in all the other processes, although the sono process showed the lowest efficiencies of decoloration and TOC removal (Figures 5 and 6). This is probably due to fewer radicals generated by H_2O_2 without iron reagents and/or the faster consumption of radicals by the RhB dyestuff degradation. A similar phenomenon was observed by Nam and co-workers.[34]

Free Iron Ions Formation in the Sono-Fe@Fe_2O_3 System. Free Fe^{2+} or Fe^{3+} ions are regarded as the efficient iron reagents in homogeneous Fenton reaction to degrade the organic pollutants. During the sono-Fe@Fe_2O_3 process, the concentration changes of free ferrous (Fe^{2+}) or ferric (Fe^{3+}) ions at different initial pH values (2 and neutral pH) were detected by atom absorption spectrometry (Figure 8). It was found that the dissolution of iron and/or iron oxide was significant at pH 2 during this process. The concentration of iron ions went up sharply from zero to 3.4 mg·L^{-1} during the first 10 min. After that, the concentration of free Fe^{2+} and Fe^{3+} ions became relatively stable, indicating the termination of the dissolution because the pH value of the solution was already 6. These free Fe^{2+} and Fe^{3+} ions in the solution would react with H_2O_2 formed under ultrasound irradiation to generate plenty of hydroxyl radicals to degrade organic pollutants. On the other hand, the concentration of free Fe^{2+} and Fe^{3+} ions did not significantly change when the initial pH value was neutral, indicating that the Fe leaching from the Fe@Fe_2O_3 core−shell nanowires was negligible at the neutral pH value. This result indicates that the application of Fe@Fe_2O_3 core−shell nanowires in the sono-Fenton system at neutral pH is very promising.

The Possible Reaction Mechanism of RhB Degradation in the Sono-Fe@Fe_2O_3 Process. In our study, when the Fe@Fe_2O_3 core−shell nanowires were introduced into the RhB solution at the initial pH 2, zerovalent iron cores would first react with H^+ because the $E_H{}^0$ of this reaction is negative to −0.440 V (eq 17). In addition, iron oxide shells would also react with H^+ (eq 18). These two reactions would consume H^+ ions, resulting in the sharp pH increase. As soon as the H^+ ions were used up, these two reactions would stop and the pH value would remain at a stable neutral value. Therefore, this novel sono-Fe@Fe_2O_3 process contained two different stages of degradation reaction: the first was in 10 min at acidic pH values; the second was after 10 min at near neutral pH value. These two stages could be easily observed in Figure 5 and the

degradation rate in the first stage was much faster than that in the second stage. Meanwhile, during these two stages the decomposition of RhB would take place not only in the bulk solution, but also on the surface of $Fe@Fe_2O_3$ core−shell "nanowires". Therefore, the degradation of RhB by this new sono-Fenton process involves not only homogeneous Fenton reaction on the basis of free iron ions and H_2O_2, but also heterogeneous Fenton reactions with Fe core/iron oxide shell and H_2O_2. First, the destruction of RhB was contributed to homogeneous sono-Fenton reactions, where H_2O_2 was sonochemically produced and Fe^{2+} or Fe^{3+} ions were leached from $Fe@Fe_2O_3$ nanowires. This reaction was reported by many investigations.[2−5,15] Second, the destruction of RhB was also contributed to a heterogeneous sono-Fenton reaction where iron oxide serves as the iron reagent. In general, this heterogeneous degradation of RhB may involve five steps: (1) mass transfer of RhB to the $Fe@Fe_2O_3$ surface from the bulk solution; (2) adsorption of RhB on the $Fe@Fe_2O_3$ surface; (3) chemical reactions at the $Fe@Fe_2O_3$ surface; (4) desorption of the products from the $Fe@Fe_2O_3$ surface; and (5) mass transfer of the products into the bulk solution. In the presence of ultrasound irradiation, turbulent flow produced by transient cavitations could enhance overall mass transport.[26,35] Moreover, acoustic cavitations broke $Fe@Fe_2O_3$ nanowires and caused the partial oxidation of their iron cores, which may increase the surface defects or active sites on the $Fe@Fe_2O_3$ "nanowires" surface. And ultrasound offered a washing effect on the surface of nanowires. Researchers found that common forms of iron oxide (goethite, hematite, magnetite, and ferrihydrite) could also catalyze the oxidation of organic compounds by H_2O_2 from pH 3 to 7,[36] which is similar to the heterogeneous degradation of RhB on iron oxide shells in our study. Valentine and Wang proposed that the surface area of the iron oxide accounted for the difference in reaction activity. They showed that the decomposition rates of H_2O_2 by goethite, ferrihydrite, and hematite were all relatively similar when normalized to surface area.[37] In our study, some fine crackings were also found on the oxide surface and more oxides were produced by the oxidation of Fe cores when $Fe@Fe_2O_3$ nanowires were exposed to ultrasound irradiation. These two factors could also promote the degradation of RhB in this sono-$Fe@Fe_2O_3$ process. Finally, the destruction of RhB might also take place via another heterogeneous sono-$Fe@Fe_2O_3$ reaction where Fe cores served as the iron reagent. It is well-known that Fe^0 is used as a reductive reagent in environmental remediation. However, recent researches suggested that the formation of Fe^{2+} on the corresponding Fe^0 surface would catalyze the decomposition of H_2O_2 to form the $^{\bullet}OH$ radical.[38,39] Degradation of organic compounds by Fe^0 was carried out in an oxidative pathway.[39−41] For instance, carbothiolate herbicide and molinate were oxidatively degraded on nanoscale zerovalent iron particles, because ferrous iron and superoxide radicals were generated on corrosion of the zerovalent iron with subsequent production of strongly oxidizing entities to degrade the trace contaminant (eqs 20 and21).[41] In this study, we thought that the Fe cores were oxidized to Fe^{2+} in air under ultrasound irradiation to react with H_2O_2 to produce $^{\bullet}OH$ on the basis of our experimental results of XRD and SEM.

$$Fe^0 + O_2 + 2H^+ \rightarrow Fe^{2+} + H_2O_2 \qquad (20)$$

$$Fe^{2+} + H_2O_2 \rightarrow Fe(OH)^{2+} + {}^{\bullet}OH \qquad (21)$$

Conclusions

This study presents the first report that $Fe@Fe_2O_3$ core−shell nanowires work as a novel iron reagent in Fenton reactions under ultrasound irradiation. It was found that this novel sono-Fenton process based on $Fe@Fe_2O_3$ nanowires showed much higher efficiency on the degradation of RhB, comparing with the Fenton processes based on Fe^0, Fe^{2+}, and Fe^{3+}. We thought that this sono-Fenton process involved homogeneous sono-Fenton reactions (Fe^{2+}, Fe^{3+}/H_2O_2) in the solution and heterogeneous sono-Fenton reactions (Fe, Fe_2O_3, Fe_3O_4/H_2O_2) on these solid surfaces. We believe the $Fe@Fe_2O_3$ nanowires are excellent materials for environmental pollutants treatment because their mass production has been realized. Moreover, we already found that $Fe@Fe_2O_3$ nanowires could efficiently work in the Fenton system at neutral pH. This cannot only extend the working pH range of the Fenton reaction, but also solve the recycle problem of traditional ionic iron reagents and avoid the dissolution of $Fe@Fe_2O_3$ nanowires in acidic solution. This attractive $Fe@Fe_2O_3$ core−shell nanowires based sono-Fenton system working at neutral pH will be reported on soon.

Acknowledgment. This work was supported by the National Science Foundation of China (Grant 20503009 and 20673041), the Outstanding Young Research Award of the National Natural Science Foundation of China (Grant 50525619), and the Open Fund of Hubei Key Laboratory of Catalysis and Materials Science (Grants CHCL0508 and CHCL06012).

Supporting Information Available: XRD patterns, SEM, and TEM images of the used $Fe@Fe_2O_3$ "nanowires". This material is available free of charge via the Internet at http://pubs.acs.org.

References and Notes

(1) Ai, Z. H.; Yang, P.; Lu, X. H. *Chemosphere* **2005**, *60*, 824−827.
(2) Voelker, B.; Sulzberger, B. *Environ. Sci. Technol.* **1996**, *30*, 1106−1114.
(3) Zepp, R. G.; Faust, B. C.; Hoigné, J. *Environ. Sci. Technol.* **1992**, *26*, 313−319.
(4) De Laat, J.; Gallard, H. *Environ. Sci. Technol.* **1999**, *33*, 2726−2732.
(5) Kwan, W. P.; Voelker, B. M. *Environ. Sci. Technol.* **2002**, *36*, 1467−1476.
(6) Chou, S.; Huang, C. *Chemosphere* **1999**, *38*, 2719−2731.
(7) Fernandez, J.; Bandara, J.; Lopez, A.; Kiwi, J. *Langmuir* **1999**, *15*, 185−192.
(8) Parra, S.; Henao, L.; Mielczarski, E.; Mielczarski, J.; Albers, P.; Suvorova, E.; Guindet, J.; Kiwi, J. *Langmuir* **2004**, *20*, 5621−5629.
(9) Bozzi, A.; Yuranova, T.; Mielczarski, J.; Kiwi, J. *Chem. Commun.* **2002**, 2202−2203.
(10) Cheng, M. M; Ma, W. H.; Li, J.; Huang, Y. P.; Zhao, J. C. *Environ. Sci. Technol.* **2004**, *38*, 1569−1575.
(11) Dhananjeyan, M.; Mielczarski, E.; Thampi, K.; Bensimon, M.; Kiwi, J. *J. Phys. Chem. B* **2001**, *105*, 12046−12055.
(12) Fernandez, J.; Dhananjeyan, M.; Kiwi, J.; Senuma, Y.; Hilborn, J. *J. Phys. Chem. B* **2000**, *104*, 5298−5301.
(13) Parra, S.; Guasaquillo, I.; Enea, O.; Mielczarski, E.; Mielczarki, J.; Albers, P.; Kiwi-Minsker, L.; Kiwi, J. *J. Phys. Chem. B* **2003**, *107*, 7026−7035.
(14) Parra, S.; Nadtotechenko, V.; Albers, P.; Kiwi, J. *J. Phys. Chem. B* **2004**, *108*, 4439−4448.
(15) Beckett, M. A.; Hua, I. *Water Res.* **2003**, *37*, 2372−2376.
(16) Quinn, J.; Geiger, C.; Clausen, C.; Brooks, K.; Coon, C.; O'hara, S.; Krug, T.; Major, D.; Yoon, W. S.; Gavaskar, A.; Holdsworth, T. *Environ. Sci. Technol.* **2005**, *39*, 1309−1318.
(17) Kim, Y. H.; Carraway, E. R. *Environ. Sci. Technol.* **2000**, *34*, 2014−2017.
(18) Sayles, G. D.; You, G.; Wang, M.; Kupferle, M. J. *Environ. Sci. Technol.* **1997**, *31*, 3448−3454.
(19) Kanel, S. R.; Greneche, J. M.; Choi, H. *Environ. Sci. Technol.* **2006**, *40*, 2045−2050.

(20) Ponder, S. M.; Darab, J. G.; Mallouk, T. E. *Environ. Sci. Technol.* **2000**, *34*, 2564−2569.
(21) Singh, J.; Comfort, S. D.; Shea, P. J. *Environ. Sci. Technol.* **1999**, *33*, 1488−1494.
(22) Qiu, S. R.; Lai, H. F.; Roberson, M. J.; Hunt, M. L.; Amrhein, C; Giancarlo, L. C.; Flynn, G. W.; Yarmoff, J. A. *Langmuir* **2000**, *16*, 2230−2236.
(23) Kanel, S. R.; Manning, B.; Charlet, L.; Choi, H. *Environ. Sci. Technol.* **2005**, *39*, 1291−1298.
(24) Bergendahla, J. A.; Thiesb, T. P. *Water Res.* **2004**, *38*, 327−334.
(25) Huang, H. H.; Lu, M. C.; Chen, J. N. *Water Res.* **2001**, *35*, 2291−2299.
(26) Huang, H. M.; Hoffmann, M. R. *Environ. Sci. Technol.* **1998**, *32*, 3011−3016.
(27) Lu, L. R.; Ai, Z. H.; Li, J. P.; Zheng, Z.; Li, Q.; Zhang, L. Z. *Cryst. Growth Des.* **2007**, *7*, 459-464.
(28) Konnann, C.; Bahnemann, D.; Hofmann, M. R. *Environ. Sci, Technol.* **1988**, *22*, 798−806.
(29) Chen, C.; Li, X.; Ma, W.; Zhao, J.; Hidaka, H.; Serpone, N. *J. Phys. Chem. B* **2002**, *106*, 318−324.
(30) Watanabe, T.; Takizawa, T.; Honda, K. *J. Phys. Chem.* **1977**, *81*, 1845−1851.
(31) Wu, J. M.; Zhang, T. W. *J. Photochem. Photobiol., A* **2004**, *162*, 171−177.
(32) Gasgnier, M.; Beaury, L.; Derouet, J. *Ultrason. Sonochem.* **2000**, *7*, 25−33.
(33) Khachatryan, A.; Sarkissyan, R.; Hassratyan, L.; Khachatryan, V. *Ultrason. Sonochem.* **2004**, *11*, 405−408.
(34) Nam, S. N.; Han, S. K.; Kang, J. W.; Choi, H. *Ultrason. Sonochem.* **2003**, *10*, 139−147.
(35) Hung, H. M.; Ling, F. H.; Hoffmann, M. R. *Environ. Sci. Technol.* **2000**, *34*, 1758−1763.
(36) Chou, S. S.; Huang, C. P. *Chemosphere* **1999**, *38*, 2719−2731.
(37) Valentine, R. L.; Wang, H. C. A. *J. Environ. Eng.* **1998**, *124*, 31−38.
(38) Voegelin, A.; Hug, S. J. *Environ. Sci. Technol.* **2003**, *37*, 972−978.
(39) Joo, S. H.; Feitz, A. J.; Waite, T. D. *Environ. Sci. Technol.* **2004**, *38*, 2242−2247.
(40) Kong, S. H.; Watts, R. J.; Choi, J. H. *Chemosphere* **1998**, *37*, 1473−1482.
(41) Joo, S. H.; Feitz, R. J.; Sedlak, D. L.; Waite, T. D. *Environ. Sci. Technol.* **2005**, *39*, 1263−1268.